IEEE Access
Multidisciplinary ⋮ Rapid Review ⋮ Open Access Journal

Received January 11, 2020, accepted January 28, 2020, date of publication February 4, 2020, date of current version February 14, 2020.

Digital Object Identifier 10.1109/ACCESS.2020.2971669

On the Design of Energy-Saving Fluid Power Converter

GUOHENG WU[1], JUNHONG YANG[2], JIANZHONG SHANG[1], ZIRONG LUO[1], TENGAN ZOU[1], AND DELEI FANG[3]

[1]College of Intelligence Science and Technology, National University of Defense Technology, Changsha 410073, China
[2]China Minsheng Drawin Intelligent Equipment Technology Company Limited, Changsha 410073, China
[3]College of Mechanical Engineering, Tianjin University of Science and Technology, Tianjin 300222, China

Corresponding author: Jianzhong Shang (shangjianzhong@nudt.edu.cn)

This work was supported in part by the National Natural Science Foundation of China under Grant 51675522, and in part by the National Natural Science Foundation of China under Grant 51705525.

ABSTRACT The high energy efficiency and lightweight are recent trends in mobile hydraulics. In this paper, a new energy-saving fluid power converter (FPC) is designed to solve the problem of low energy conversion efficiency in hydraulic systems with variable load. The FPC is a kind of hydraulic transformer, it is similar to the DC transformer in working principle. Pulse width modulation (PWM) signal is used to control the high-speed on-off valves, and the high-speed on-off valve can switch supply ports between different pressure oil sources to achieve the adjustment of the FPC's output. The FPC's mathematical principle is analyzed in this paper, the influence of the friction between the inertial mass and the conversion cylinder on the system efficiency is studied. The influence of the PWM signal frequency, conversion cylinder cross-sectional area and inertial mass on the characteristics of FPC system is deduced. The results of the analysis are validated by Matlab/Simulink, and suggestions of selecting the design parameters of FPC are provided.

INDEX TERMS Energy efficiency, energy-saving, fluid power converter, hydraulic transformer, simulation.

I. INTRODUCTION

The high ratio of power to weight is an important feature of hydraulic systems. With the pursuit of higher drive performance, hydraulic systems with more compact, lighter weight and higher energy efficiency have bright application prospects in mobile hydraulic robots and industrial hydraulic systems [1], [2].

Hydraulic servo valves are key components of hydraulic systems, especially of the high performance hydraulics. One of the main deficiencies of traditional servo valves is the loss of throttling during adjustment, which reduces energy efficiency. In fact, the efficiency of common valve-controlled hydraulic systems is relatively low. For example, the efficiencies of excavators using conventional valve-controlled hydraulic systems are typically below 40%, and the throttling effect is an important negative cause [3]–[5]. For variable-load multi-actuator hydraulics, this deficiency will be amplified and present a huge challenge to the system regarding cooling and durability. Driving the hydraulic fluid directly through the controllable variable pump (a pump with variable displacement) is a method to avoid throttle losses. However, the variable displacement pump is bulky and expensive, and providing a separate variable control pump for each actuator will complicate and cumber the hydraulic system.

The single-pump multi-actuator hydraulic system has the advantages of simple structure, high power density and light weight, which is very suitable for high-performance multi-degree-of-freedom drive systems. And most hydraulic robots have outstanding power or output torque performance. But the hydraulic system's efficiency have a very important impact on the performance of the robot, energy efficiency and endurance are important indicators of the powertrain. Therefore, the development of high efficiency single-pump multi-actuator hydraulic system is of interest [6].

A. DEVELOPMENT STATUS OF HYDRAULIC TRANSFORMER

The hydraulic transformer is a hydraulic energy regulating device that adjusts the hydraulic output to match the load in an unthrottled manner, which can effectively reduce the energy loss caused by the large difference between the pump pressure and the load pressure. With the development of digital control technology, using digital hydraulic components to replace traditional control valves has become an important

The associate editor coordinating the review of this manuscript and approving it for publication was Hamid Mohammad-Sedighi.

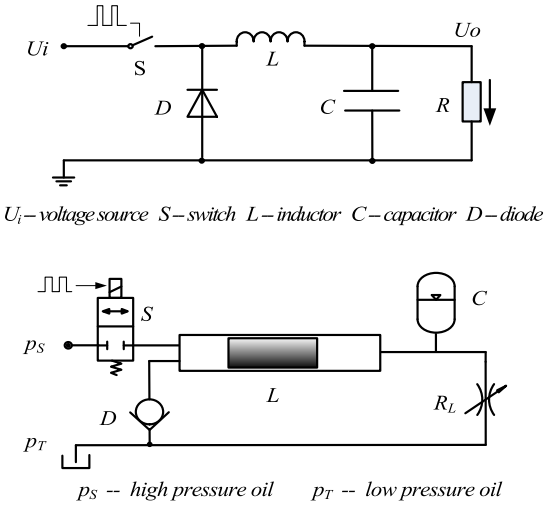

FIGURE 1. The Buck DC transformer and the FPC.

means to improve the energy efficiency of hydraulic systems [7]–[13]. Guglielmino and Helmut Kogler proposed a hydraulic transformer, which uses high-frequency switching valves, slender tubing and accumulator analog DC transformers. The system output pressure and flow can be adjusted by PWM signal [14]–[16].

Kyoung Kwan Ahn of Ulsan University, Korea, et al. use wheel and hydraulic motor to form the inertial component of hydraulic the transformer and cooperate with large-capacity accumulators for energy recovery and release [17]–[19]. Zhejiang University Fluid Power Transmission and Control Laboratory proposed an inertial hydraulic transformer. A flywheel and a hydraulic motor form the inertial component, the high frequency switch valve can be controlled by the PWM signal to adjust the output pressure [9], [20]. Due to size and weight constraints, these two transformers can be used in large engineering hydraulics, but are difficult to use in small hydraulic robots.

The hydraulic transformer (HT) can also be configured by connecting two pump/motors mechanically. IHT is a breakthrough product made by Innas Company [21], its output pressure is varied by regulating the angle of the port plate manually, and some control researches were carried out [22]. However, this HT is manually controlled and it is difficult to meet the automatic requirements. Then, Wei Shen proposed a new type of HT, which is integrated with a swing vane motor to control the angular displacement of the port plate directly [23]. DHT is a digital hydraulic transformer, the device has a number of working oil chambers with different cross-sectional areas, and each working chamber is controlled by a two-position three-way valve. By combining different working chambers, the output pressure can be discretely adjusted [24].

Based on the principle of the Buck DC transformer, Xue Yong designed the FPC system. The DC transformer can control output voltage through PWM technology with low power consumption, as shown in Fig.1. The inductor transfers the stored energy to the load, and the capacitor smoothes

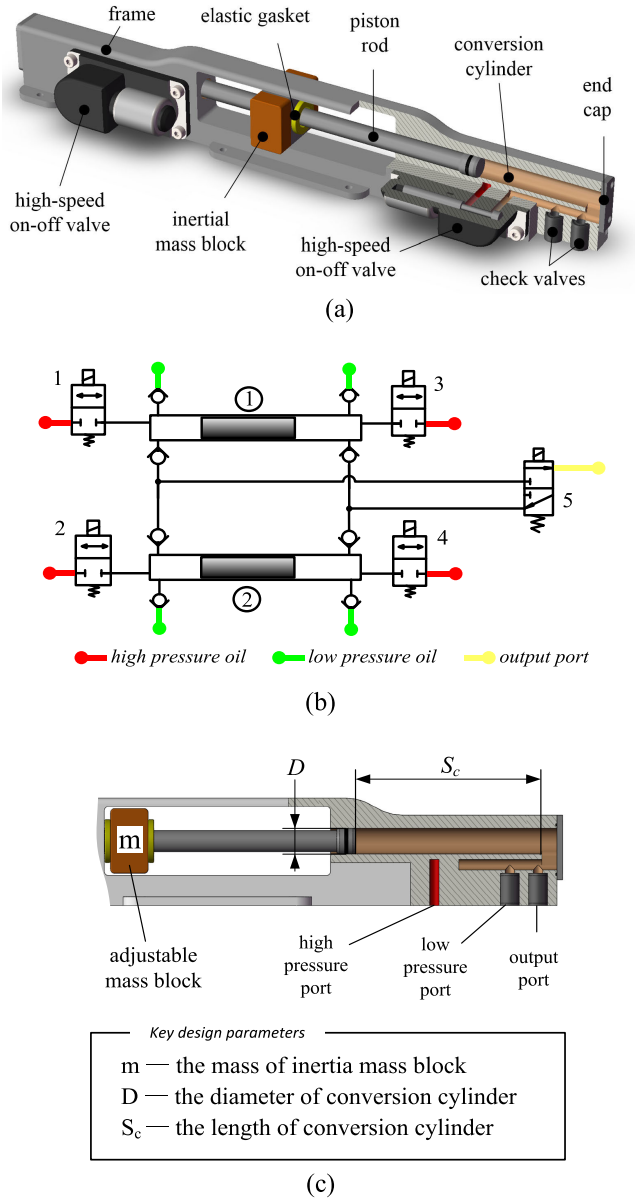

FIGURE 2. The new FPC device: (a) A partial sectional view of the inertial device, one FPC contains two inertial devices, (b) The schematic of new FPC system, (c) The inertial device's key design parameters.

the voltage. In FPC, the inertial mass corresponds to the inductance component, the accumulator corresponds to the capacity component, and the high-speed on-off valve is used to switch the conversion state. Since the high-speed on-off valves almost operated in fully open or fully closed state, the pressure loss and energy loss is low [25].

B. INTRODUCTION OF THE NEW FPC

The improved FPC is designed as shown in Fig.2.

The FPC is consisting of two inertial devices, a two-position three-way valve, 4 high-speed on-off valves and 8 check valves. Compared with Xue Yong's FPC design, the new design simplifies the principle and structure. The main components of the inertial device include two

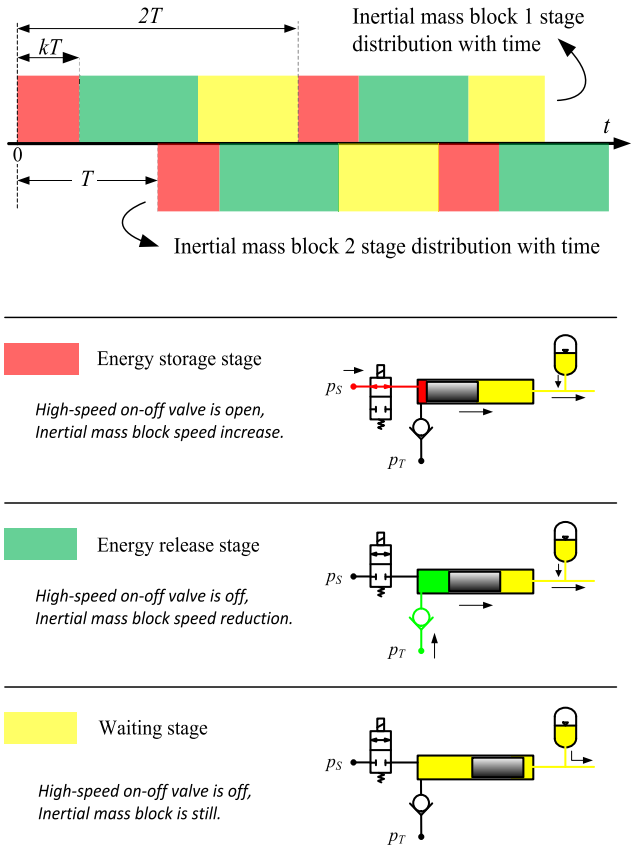

FIGURE 3. FPC working stage distribution.

high-speed on-off valves, the inertial mass, the elastic gasket, the piston rod, the conversion cylinders, check valves and the end cap. The inertial mass, the piston rod and the elastic gasket together form the inertial mass module. The mass block is fixed with piston rods and can only reciprocate in the axial direction of the conversion cylinder. The elastic gasket is used to avoid rigid collision between the mass block and the frame. The inertial device's key design parameters are shown in Fig.2(c).

The FPC system's work process consists of three stages: (a) energy storage stage, (b) energy release stage, (c) waiting stage. The distribution of working stages of the FPC over time is as shown in Fig.3. When the high-speed on-off valve port is opened and the pressure of the high-pressure oil is higher than the load pressure, the high-pressure oil accelerates the inertial mass block, and stores the excess energy as the kinetic energy of the inertial mass. When the high-speed on-off valve is closed, the inertia of motion will cause the inertial mass and the piston rod to continue to slide, the hydraulic oil is squeezed from the conversion cylinder to the load port, and the stored kinetic energy release and re-converted into hydraulic energy. The waiting stage is the stationary stage in which the inertial mass decelerates to zero, neither high pressure oil nor low pressure oil enters the conversion cylinder. The three stages are cyclically switched in time sequence. Above the time axis is the stage distribution of the inertial mass 1, and below the time axis is the stage distribution of the

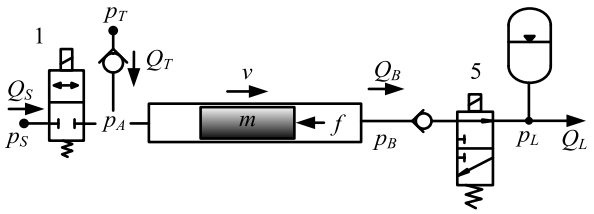

FIGURE 4. FPC mathematical model diagram.

inertial mass 2. The phase difference between the two inertial components is 180°. The duration of energy storage stage is kT (k is the PWM wave duty cycle), the duration of energy release stage and waiting stage is determined by factors such as low pressure oil pressure and load pressure. The output of the new FPC can be controlled by changing the duty cycle k.

II. FPC CONTROL MECHANISM

According to the working principle shown in Fig.3, the inertial device ① and the inertial device ② operate in the same manner, but with different phases. Therefore, it is only necessary to analyze an inertial device's situation. Fig.4 shows an analytical diagram of the inertial device ①.

The FPC has the same seal structure with the traditional linear hydraulic cylinder. Under normal circumstances, the FPC leakage is extremely limited and this article regards the FPC system as an ideal leak-free device.

The load of the FPC system proposed in Xue Yong's article is a throttle valve. When changing the size of the throttle port, it not only changes the valve's flow, but also affects the load pressure. This can easily lead to the wrong understanding that the FPC can directly control the output pressure. In the actual hydraulic system, the output pressure of is always determined by the load. For example, if the load of the FPC is a common hydraulic cylinder instead of a throttle, the FPC cannot change the output pressure.

The acceleration and deceleration phases of the inertial mass correspond to the high pressure oil supply phase and the low pressure oil supply phase respectively. When the PWM signal is high level, the high-speed on-off valve opens and high pressure oil enters the left conversion chamber to push the inertial mass to accelerate. When the PWM signal is low level, the low pressure oil enters the left conversion chamber, as the low pressure oil pressure is lower than the load pressure, the inertial mass is decelerated.

When the PWM signal is high level, the inertial mass acceleration can be derived:

$$a_S = \frac{(P_A - P_B)A - f}{m} \tag{1}$$

where A is the cross-sectional area of conversion cylinders, f is the friction force between the piston rods and conversion cylinders, and m is the mass of the inertial mass block and the piston rod. When the PWM signal is low level, the inertial mass acceleration can be derived:

$$a_T = \frac{(P_B - P_A)A + f}{m} \tag{2}$$

When the system flow is smaller than the rated flow, the pressure drop caused by switch valve and check valve is small. Therefore, ignore the pressure drop caused by switch valve and check valves, set $P_B = P_L$; when high-speed on-off valve 1 is open, set $P_A = P_S$; when high-speed on-off valve 1 is close, set $P_A = P_T$, and following equations can be derived:

$$a_S = \frac{(P_S - P_L)A - f}{m}, \quad a_T = \frac{(P_L - P_T)A + f}{m} \tag{3}$$

where P_L is the load pressure, P_S and P_T are high pressure oil pressure and low pressure oil pressure, respectively. In normal working conditions, the inertial mass accelerates from a standstill, then reaches the maximum speed $v_{\max}$, and then decelerates to a standstill again. Suppose that the period of the PWM signal is T, the duty cycle of the PWM signal is k, so the time of high level in a period is $t_S = kT$, which is also the high pressure oil supply time and the acceleration time in a cycle. Suppose the deceleration time is $t_T = it_S = ikT$, and following equations can be derived:

$$v_{\max} = \int_0^{t_S} a_S dt = \int_0^{t_T} a_T dt \tag{4}$$

Ignore the pressure drop caused by switch valve and check valve, the movement of the mass can be regarded as a uniform acceleration movement, and then the following equation can be derived:

$$i = \frac{t_T}{t_S} = \frac{a_S}{a_T} = \frac{(P_S - P_L)A - f}{(P_L - P_T)A + f} \tag{5}$$

The acceleration distance of the inertial mass is S_a, the deceleration distance is S_d, and the total distance is S. Then employing equation (5) to give

$$S_a = \frac{1}{2} v_{\max} t_S = \frac{1}{2} a_S t_S^2 = \frac{1}{2} a_S k^2 T^2 \tag{6}$$

$$S_d = \frac{1}{2} v_{\max} t_T = \frac{1}{2} a_T t_T^2 = \frac{1}{2} a_T i^2 k^2 T^2 \tag{7}$$

$$S = S_a + S_d = \frac{1}{2} v_{\max}(t_S + t_T) = \frac{1}{2}(1+i) a_S k^2 T^2 \tag{8}$$

According to the working principle of the FPC system shown in Fig.4, Q_S and Q_T are respectively the high pressure oil flow rate and low pressure oil flow rate which are engaged in work. The following equations are exist:

$$Q_S = \frac{S_a A}{T}, \quad Q_T = \frac{S_d A}{T} \tag{9}$$

$$\frac{Q_S}{Q_T} = \frac{S_a}{S_d} = \frac{1}{i} = \frac{(P_L - P_T)A + f}{(P_S - P_L)A - f} \tag{10}$$

Employing Eqs. (9) and (10), the output flow of the FPC is obtained:

$$Q_L = Q_S + Q_T = \frac{SA}{T} = \frac{1}{2}(1+i) a_S k^2 TA \tag{11}$$

It can be seen from equation (10) that changing the duty cycle k cannot change the proportion of high pressure oil and low pressure oil. The proportion of high pressure oil and low pressure oil is only related to i, which means the proportion only changes with the load pressure P_L when P_S, P_T, A, f and other parameters of the hydraulic system are constant. And equation (11) shows the PWM duty cycle k can adjust the output flow of the FPC, and the output flow is proportional to the square of the duty cycle k. Therefore, the FPC can control the output flow by changing the duty cycle, not directly control the output pressure.

III. EFFECT OF FRICTION ON FPC CONVERSION EFFICIENCY

According to the principle of energy conservation, the following equation can be drawn:

$$P_S Q_S + P_T Q_T = P_L(Q_S + Q_T) + \Delta w \tag{12}$$

where Δw is the friction loss per unit time. Since the output hydraulic oil is all extruded by the inertial mass module, the following equations are obtained:

$$\Delta w = \frac{Q_L}{A} f \tag{13}$$

$$P_L = \frac{P_S Q_S + P_T Q_T}{Q_S + Q_T} - \frac{f}{A} \tag{14}$$

If all of the output oil is supplied with high pressure oil, after filtering and compensation, the maximum load pressure that the FPC can match is P_m.

$$P_m = P_S - \frac{f}{A} \tag{15}$$

Then the conversion efficiency of the FPC can be expressed as the following equation:

$$\eta = 1 - \frac{\Delta w}{P_S Q_S + P_T Q_T} = 1 - \frac{Q_L}{P_S Q_S + P_T Q_T} \cdot \frac{f}{A} \tag{16}$$

In order to improve the efficiency of the FPC, it is necessary to minimize the pressure loss caused by friction or increase the cross-sectional area of the conversion cylinder.

If the O-ring is taken for sealing between the piston rod and the conversion cylinder, it must be made to have a certain amount of compression deformation. The stress and strain of the O-ring involved in the dynamic seal are mainly related to the following two aspects: The pre-compressed and the working pressure of hydraulic oil p. The total frictional force caused by the O-ring on the hydraulic cylinder piston can be expressed as follows [26]:

$$f = f_1 + f_2 = \frac{\mu \pi D w}{1 - \gamma^2}[0.2\pi eE + \gamma(1+\gamma)p] \tag{17}$$

where f_1 is the friction caused by the pre-compression, f_2 is the friction caused by the hydraulic oil, μ is the friction coefficient between the sealing ring and the cylinder, D is the cylinder diameter, w is the contact width of the sealing ring and the cylinder, e is the pre-compression rate of the O-ring, E is the elastic modulus of the sealing ring, γ is the Poisson's coefficient, p is the hydraulic oil pressure. Employing equation (16) and equation (17), the conversion efficiency

becomes

$$\eta = 1 - \frac{Q_L}{P_S Q_S + P_T Q_T} \cdot \frac{4\mu w}{(1-\gamma^2)D}[0.2\pi eE + \gamma(1+\gamma)p] \tag{18}$$

From Equation (18), it can be concluded that the design of inertial mass module affects the FPC efficiency. Increasing the conversion cylinder diameter can improve the FPC energy efficiency. In addition, it can be found that if the FPC absorbs more high-pressure hydraulic oil, the conversion efficiency will be higher.

IV. EFFECT OF THE INERTIAL MASS ON FPC

The inertial mass is a key part of FPC, its mass does not only affect the weight of the FPC, but also affects its performance. Xue Yong's paper only set a value for the inertial mass, not point out the design basis of the inertial mass. This section will explore the appropriate value for the mass of the inertial mass module.

If the inertial mass is increased, the acceleration of the inertial mass block will decrease and the total distance S will decrease. If the inertial mass is reduced, the acceleration of the inertial mass will increase accordingly, and the total distance S will increase. In order to avoid collision between the inertial mass block and the conversion cylinder, the length of the conversion cylinder should be greater than the total distance S.

$$S = \frac{1}{2}(1+i)a_S k^2 T^2 = \frac{(P_S - P_L)A - f}{2m} \cdot \frac{(P_S - P_T)A}{(P_L - P_T)A + f} k^2 T^2 \tag{19}$$

As S is a function of $x = \begin{bmatrix} P_L \\ k \end{bmatrix}$, and $P_T < P_L < P_S$, $0 < k \leq 1$.

The Kuhn-Tucker condition is used to determine its maximum value. The problem is translated as follows:

$$\begin{cases} \min f(x) = S = \dfrac{(P_S - P_L)A - f}{2m} \cdot \dfrac{(P_S - P_T)A}{(P_L - P_T)A + f} k^2 T^2 \\ s.t.\ g_1(x) = (1+i)k - 2 \leq 0 \\ g_2(x) = k - 1 \leq 0 \\ g_3(x) = -k < 0 \\ g_4(x) = P_L + P_T < 0 \\ g_5(x) = P_L - P_S < 0 \end{cases} \tag{20}$$

After testing, $f(x)$ and $g_i(x)$ are continuous and differentiable in the constraint range. In addition, $f(x)$ and $g_i(x)$ are convex functions.

Set x^* as the K-T point, and introduce Lagrange multiplier to the constraint, then obtain the following K-T condition:

$$\begin{cases} \nabla f(x^*) + \sum_{i=1}^{5} \lambda_i \nabla g_i(x^*) = 0 \\ \lambda_1 \nabla g_1(x^*) = \lambda_2 \nabla g_2(x^*) = \lambda_3 \nabla g_3(x^*) = \lambda_4 \\ \nabla g_4(x^*) = \lambda_5 \nabla g_5(x^*) = 0 \\ \lambda_1, \lambda_2, \lambda_3, \lambda_4, \lambda_5 \geq 0 \end{cases}$$

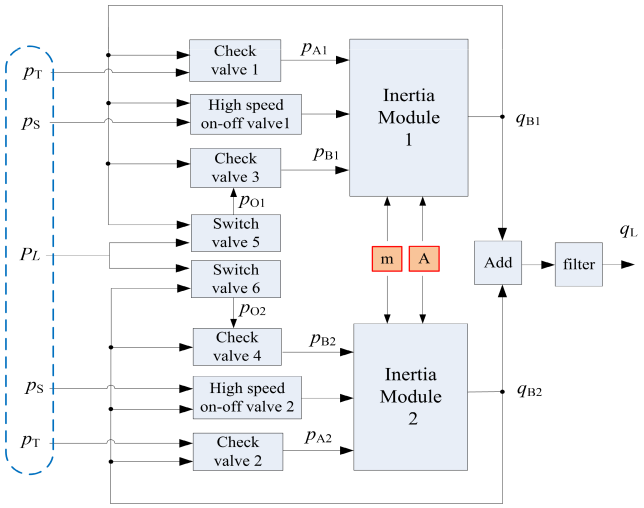

FIGURE 5. The Simulink Model of the FPC: P_S, P_T, P_L are variable input parameters, m and A are the main design parameters that are not easy to change, which is the focus of this paper.

Obviously, $\lambda_3 = \lambda_4 = \lambda_5 = 0$, the results are as follows:

(1) When $\lambda_1 > 0, \lambda_2 > 0$, no solution;
(2) When $\lambda_1 > 0, \lambda_2 = 0$,

$$x^* = \begin{bmatrix} \frac{1}{2}(P_S + P_T) - \frac{f}{A} \\ 1 \end{bmatrix}, \quad S_{\max} = \frac{1}{2}(P_S - P_T)\frac{AT^2}{m} \tag{21}$$

(3) When $\lambda_1 = 0, \lambda_2 > 0$, no solution;
(4) When $\lambda_1 = 0, \lambda_2 = 0$, no solution;

That is, when $k = 1, P_L = (P_S + P_T)/2\text{-f}/A$, the total distance S reaches its maximum value $S_{\max}$. From the deduction result, the value of $S_{\max}$ is independent of friction f. Therefore, the length of the conversion cylinder is proportional to the pressure difference $(P_S - P_T)$, the cross-sectional area A of the conversion cylinder and the square of the PWM signal period T^2, and inversely proportional to the mass of the inertial mass module.

V. SIMULATION

In order to analyze the characteristics of the FPC, a simulation model is built in MATLAB/Simulink according to the working mechanism of the FPC, as shown in Fig.5. All sub-module models are based on the mathematical model of each component.

High-speed On-Off valves, switching valves and check valves can be mathematically simplified to standard holes in simulation, their dynamic characteristics can be expressed by Bernoulli small hole equation [27], which can be described as follows.

$$q_v = \frac{Q_N}{\sqrt{p_N}}\sqrt{\Delta p} \tag{22}$$

where q_v is the flow through the valve, Δp is the pressure drop, Q_N is the flow of the valve at the rated pressure drop p_N.

TABLE 1. Simulation parameters of FPC system.

Notation	Parameter	Valve
P_S	supply pressure	16MPa
P_T	Tank pressure	1MPa
B	Bulk modulus of the fluid	14000 bar
ρ	Density of the fluid	875 kg/m3
Q_{NS}	Reference flow of high-speed on-off valve	20L/min@5bar
Q_{NC}	Reference flow of check valve	60L/min@5bar
f	Friction between the inertial mass and conversion cylinder	0N
γ	Polytropic index	1.4

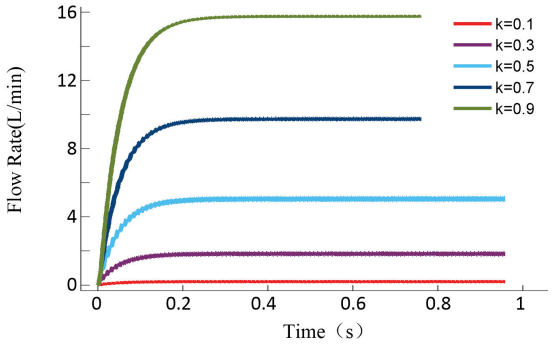

FIGURE 6. FPC simulation flow output curves under different input k.

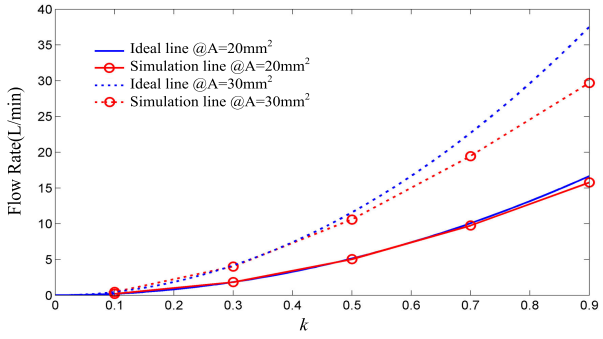

FIGURE 7. The results of the FPC's calculation and FPC's simulation at different k.

The simulation parameters of the FPC are given in Table 1, where the friction is negligible compared to hydraulic thrust, and suppose the valve response is fast enough.

In order to validate whether the output flow of the FPC conforms to $Q_L = 0.5(1+i)a_S k^2 T$, set the system load pressure to 8 Mpa and the PWM control signal frequency to 100Hz. The simulation results are shown in Fig.6.

In two simulation experiments, the cross-sectional area of the conversion cylinder was set to 20 mm^2 and 30 mm^2, and the output flow of the FPC was recorded. Comparing the simulation results with the ideal calculation results, and the differences are shown in Fig.7.

Fig. 7 represents the flow results of the FPC's calculation and simulation for the period $T = 0.01s$. It shows that the output flow increases with the control variable k. There is some deviation between the simulation results and the ideal

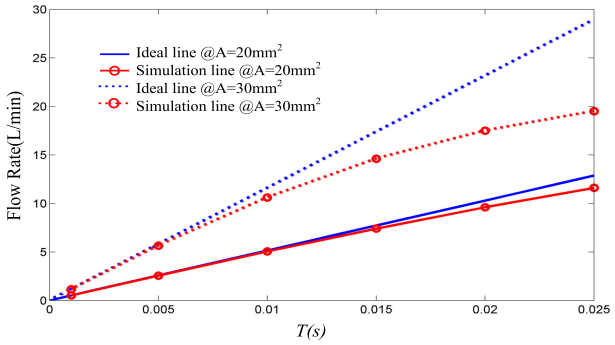

FIGURE 8. The results of the FPC's calculation and FPC's simulation at different T.

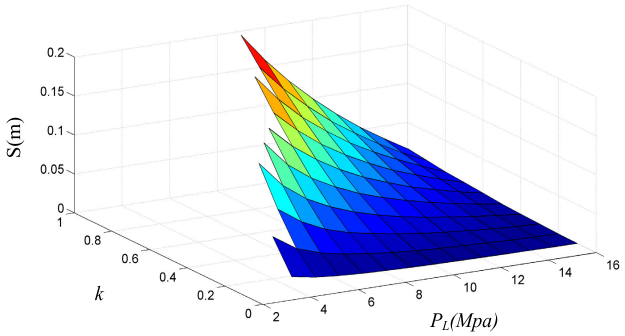

FIGURE 9. Simulation results of S under different P_L and k (the PWM signal period T=0.01s, the mass of the inertial mass m=0.1kg, conversion cylinder cross-sectional area A=30mm^2).

calculation results because the throttling effect of the switching valve and the check valve is neglected in the theoretical derivation in order to simplify the calculation. This simplification has a certain impact on the output flow of the FPC. Moreover, this deviation will increase as the output flow increase, so the above derivation equations are only applicable to the normal state where the output flow is less than rated flow.

The period of the PWM signal also have a similar effect on FPC. As shown in Fig.8, set the control variable k to 0.5, as the period T increases, the output flow of the FPC increases, but there is a deviation between the ideal lines and the simulation lines. When the output flow of the FPC is small, the simulation results are in good agreement with the ideal calculation results. As the output flow of the FPC increases, the deviation increases.

From equation (21), the total distance S of the inertial mass block reaches a maximum at $P_L = (P_S + P_T)/2 - f/A$. In order to validate the correctness of the derivation result, simulations were performed under different control variables and different load pressures. Since the Simulink model ignores the friction and throttling loss of the system, the total distance S of the inertial mass should reaches its maximum value when the load pressure at $(P_S + P_T)/2$. The simulation result is shown in Fig.9, when $k \approx 1, P_L \approx 8.5Mpa$, the total distance S reaches the maximum value, which is consistent with the derivation result of equation (21).

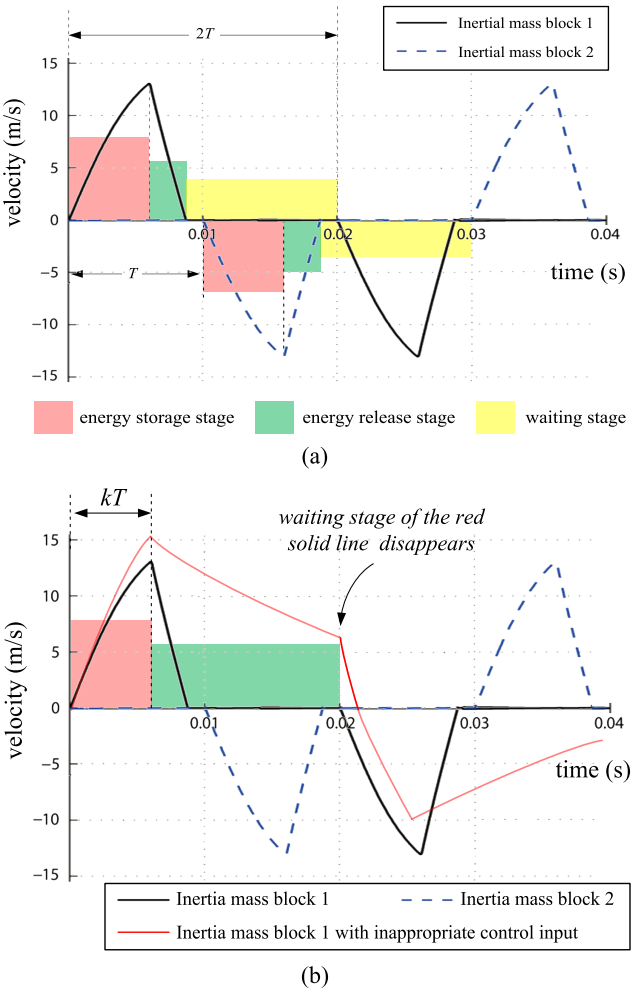

FIGURE 10. Ideal motion and undesirable situation of inertial mass-block in FPC. (a) Ideal velocity-time curves. (b) An undesirable situation of inertial mass block.

A large area in the left side of the figure does not show values for S in a certain range of k and P_L because the control input k value in this area do not allow a proper operation of the FPC. As shown in Fig.10(a), there are ideal velocity-time curves of two inertial mass blocks. Above the time axis is the stage distribution of the inertial mass 1 over time, and below the time axis is the stage distribution of the inertial mass 2 over time. The black solid line represents the ideal motion of inertia mass-block 1, the blue dotted line represents the ideal motion of inertia mass-block 2. The inertial mass block velocity increases during the energy storage stage, reaches a maximum at the junction of the energy storage stage and the energy release stage, and drops to zero at the end of the energy release stage.

Above the time axis is the stage distribution of the inertial mass 1 over time, and below the time axis is the stage distribution of the inertial mass 2 over time. The phase difference between the two inertial component control inputs is 180°. The duration of energy storage stage is kT.

The red solid line in Fig.10(b) shows an undesirable situation of inertial mass block. When the load pressure P_L becomes smaller and the control input k is not changed, the deceleration of the inertial mass becomes smaller, which means that more time is needed to wait the mass block decelerate to zero and the energy release stage grows. When the load pressure is not big enough to stop the inertial mass block in limited time, the waiting stage will disappear and the residual energy of the inertial mass block will affect the next cycle. The value of k is limited according to P_L to avoid similar problems with FPC.

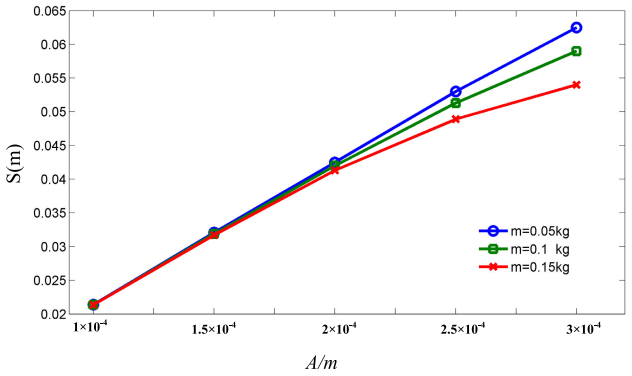

FIGURE 11. Simulation results of FPC under different A/m.

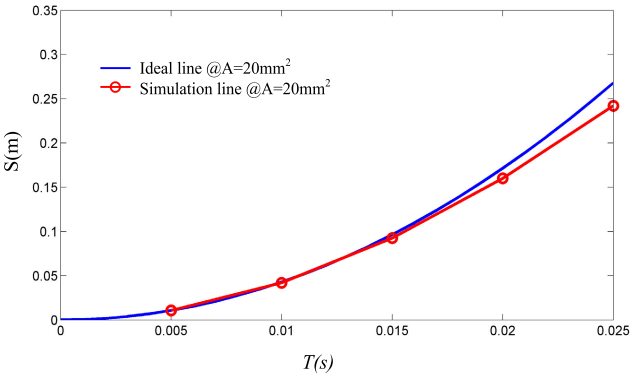

FIGURE 12. Simulation results of FPC under different T.

In equation (21), the total distance S of the inertial mass is linearly related to A/m. With different A/m values, the corresponding simulation results are shown in Fig.11. (Where the load pressure $P_L = 8Mpa$, PWM signal period $T = 0.01s, k = 0.5$).

And the total distance S of the inertial mass is linearly related to T^2. With different T values, the corresponding simulation results are shown in Fig.12. (Where the load pressure $P_L = 8Mpa$, the inertial mass $m = 0.1kg$, conversion cylinder cross-sectional area $A = 20mm^2, k = 0.5$).

VI. FPC PARAMETER DESIGN

According to the above analysis, factors such as the PWM signal period, the mass of the inertial mass module, and the cross-sectional area of the conversion cylinder have an important impact on the performance of FPC. The key design parameters of the FPC should be optimized for different applications.

TABLE 2. Main Performances of different hydraulic high speed switch valves.

The type of valve	Pressure (Mpa)	flow (L/min)	Switch Time (ms)	Power Consumption (W)
lectromagnet ball valve	10	2.5~3.5	1~5	15~300
Force motor ball valve	20	1.2	0.8	0.8
Electromagnet cone valve	3~20	4~20	2~3.4	15
Electromagnet slide valve	7~20	10~13	3~5	15
Piezoelectric crystal slide valve	5	0.65	0.5	400

A. THE SELECTION OF PWM SIGNAL FREQUENCY

The high-speed on-off valve has the following characteristics [28]: (1) the control signal frequency has little effect on the flow, but the linearity of the valve increases with the frequency increasing; (2) The higher the signal frequency, the greater the range of the valve's dead zone and the valve's saturation zone. The higher the switching frequency of the high-speed on-off valve in the FPC system, the higher the control precision of the FPC, but the control range will be reduced due to the increase of the dead zone and the saturation area. In addition, according to the working principle of FPC, high-speed switching valve operating mode will bring output flow fluctuations to the FPC system. Therefore, on the one hand, the PWM signal frequency should match the response capability of the high-speed on-off valve. On the other hand, in order to improve the control accuracy of the FPC system, high-speed on-off valve with high-speed response capability should be selected.

But the current hydraulic high-speed on-off valve cannot achieve the high flow and high frequency at the same time. For example, the current high-speed on-off valve cannot simultaneously achieve following performance: flow rate is about $10L/\text{min}$, working pressure up to $20Mpa$, frequency response up to 200Hz [29]. Table 2 lists the main performance of hydraulic high-speed on-off valves with different constructions.

The principles of these high-speed on-off valves vary, and the costs vary widely. When the rated flow rates of different high-speed on-off valves are the same, the higher the frequency of the valve, the higher the manufacturing difficulty and the cost. Because there are 4 high-speed on-off valves and a two-position three-way valve in the new FPC, the cost factor should be taken into account.

Fig.13 is a simplified diagram showing the general trend of the rated flow rate and cost of a high-speed on-off valve over a range of frequencies. The rated flow rate of the high-speed on-off valve will decrease as the response frequency increases, but the cost will increase as the response frequency increases.

Therefore, according to the FPC application requirements, the maximum output flow Q_m needs to be determined first, and the shadow part of the figure is the area that able to satisfy the flow demand. If the application has a high requirement

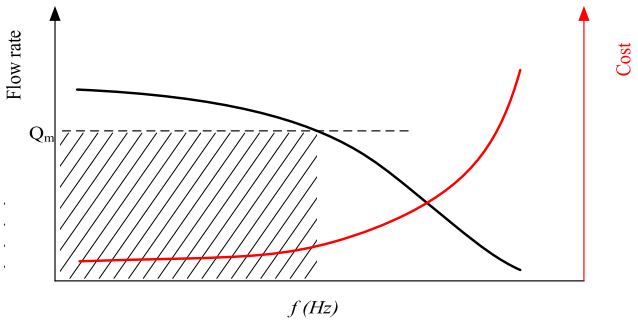

FIGURE 13. Rated flow rate and cost of the high-speed on-off valve at different response frequencies.

TABLE 3. Parameter of FPC under different applications.

FPC design constraints		Weight constraint	
		Requires small weight	Weight can be large
Size constraint	Requires small size	Reduce the diameter D of the conversion cylinder	Set the mass of inertial mass, then calculate the diameter D
	Size can be large	Set the length of the conversion cylinder first, then calculate the diameter D	Increase the diameter D of the conversion cylinder

for control accuracy, the higher frequency region of the shaded area should be considered. On the contrary, if the FPC application has no requirement about precision, the lower frequency region of the shaded area can be considered to reduce cost.

B. DESIGN OF INERTIAL MASS AND DIAMETER OF CONVERSION CYLINDER

When the frequency of the input PWM signal is determined, the minimum length $S_{\max}$ of the conversion cylinder, the mass m of the inertial mass and the cross-sectional area A of the conversion cylinder satisfy the following equation:

$$\frac{S_{\max}m}{A} = \frac{4S_{\max}m}{\pi D^2} = \frac{1}{2}(P_S - P_T)T^2 \tag{23}$$

Therefore, when the size of the FPC is required to be small in some cases, it is necessary to increase the value of $4m/\pi D^2$ in order to make the length $S_{\max}$ shorter. And it is preferable to increase the value of $4m/\pi D^2$ by reducing the diameter D of the conversion cylinder. (Although increasing the diameter D of the conversion cylinder can increase the efficiency of the system to some extent, it will increase the mass of the inertial mass a lot.

When the weight of the FPC is required to be small in some cases, it is necessary to increase the value of $4S_{\max}/\pi D^2$ in order to make the mass m of the inertial mass less. Since $S_{\max}$ is proportional to the square of the diameter of

the conversion cylinder, the longest length of the conversion cylinder that can be accepted should be determined first, and then calculate the diameter D of the conversion cylinder.

In summary, FPC parameters need to be targeted according to different applications, as shown in Table 3.

VII. SUMMARY

This paper analyzed the PWM control mathematical principle of FPC system, the output flow of the system can be changed by changing the duty cycle of PWM signal. The influence of the friction between the inertial mass and the conversion cylinder on the system efficiency is studied, and the output efficiency can be improved by increasing the diameter of the conversion cylinder. The influence of PWM signal period, conversion cylinder cross-sectional area and the mass of the inertial mass on the characteristics of FPC is deduced. And based on MATLAB/Simulink model, the effects of FPC key design parameters are simulated and validated. Finally, suggestions for FPC design parameters are proposed for different applications.

Design and simulation are only part of the verification of the new FPC. This article only studies and discusses the key parameters of the design, such as hydraulic flow resistance analysis, heat loss analysis, manufacturing process and other research will continue. In addition, a more direct and effective method is to conduct prototype testing. Although experimental verification is expensive and time-consuming, we plan to complete a simple prototype first and then start prototype research and testing.

REFERENCES

[1] K. Suzumori and A. A. Faudzi, "Trends in hydraulic actuators and components in legged and tough robots: A review," *Adv. Robot.*, vol. 32, no. 9, pp. 458–476, May 2018.

[2] S. Seok, A. Wang, M. Yee Chuah, D. Otten, J. Lang, and S. Kim, "Design principles for highly efficient quadrupeds and implementation on the MIT Cheetah robot," in *Proc. IEEE Int. Conf. Robot. Autom.*, May 2013, 3307 3312.

[3] J. I. Yoon, A. K. Kwan, and D. Q. Truong, "A study on an energy saving electro-hydraulic excavator," in *Proc. ICCAS-SICE*, 2009, pp. 3825–3830.

[4] A. Bedotti, F. Campanini, M. Pastori, L. Riccò, and P. Casoli, "Energy saving solutions for a hydraulic excavator," *Energy Procedia*, vol. 126, no. 2, pp. 1099–1106, Sep. 2017.

[5] D. W. Kong, K. L. Zhao, and N. S. Xu, *Hydraulic Excavator*. Beijing, China: Chemical Industry Press, 2007.

[6] F. F. Xie, D. F. Hao, B. Liu, and J. A. Zhang, "Design of electro—Hydraulic servo control system for lower limb external skeleton," *Mech. Des. Manuf. Eng.*, vol. 43, no. 12, pp. 20–23, 2014.

[7] G. S. Payne, A. E. Kiprakis, M. Ehsan, W. H. S. Rampen, J. P. Chick, and A. R. Wallace, "Efficiency and dynamic performance of digital displacement hydraulic transmission in tidal current energy converters," *Inst. Mech. Eng., A, J. Power Energy*, vol. 221, no. 2, pp. 207–218, Mar. 2007.

[8] W. W. Wang, J. Song, L. Li, and H. Z. Li, "The proportion function of high speed on-off valve under high frequency PWM control," *J. Tsinghua Univ.*, vol. 51, no. 5, pp. 715–719, 2011.

[9] F. Wang, L. Gu, and Y. Chen, "A continuously variable hydraulic pressure converter based on high-speed on–off valves," *Mechatronics*, vol. 21, no. 8, pp. 1298–1308, Dec. 2011.

[10] Z. Y. Zhang, B. Sun, and Y. F. Huang, "High-speed on-off valve position control method," *Mach. Tool Hydraul.*, vol. 33, no. 5, pp. 126–128, 2005, doi: 10.3969/j.issn.1001-3881.2005.05.054.

[11] J. X. Hu, J. J. Li, and D. Q. Zhong, "High-speed on-off valve and its development trend," *Develop. Innov. Electromech. Products*, vol. 22, no. 2, 60–62, 2009.

[12] H. Kogler and R. Scheidl, "Two basic concepts of hydraulic switching converters," in *Proc. 1st Workshop Digit. Fluid Power*, Tampere, Finland, 2008, pp. 113–128.

[13] P. Wang, S. Kudzma, D. N. Johnston, A. Plummer, and A. J. Hillis, "The influence of wave effects on digital switching valve performance," in *Proc. 4th Workshop Digit. Fluid Power*, Linz, Austria, 2011. [Online]. Available: https://researchportal.bath.ac.uk/en/publications/the-influence-of-wave-effects-on-digital-switching-valve-performa

[14] E. Guglielmino, C. Semini, Y. Yang, D. Caldwell, H. Kogler, and R. Scheidl, "Energy efficient fluid power in autonomous legged robotics," in *Proc. ASME Dyn. Syst. Control Conf.*, vol. 2, Jan. 2009, pp. 1–8.

[15] E. Guglielmino, C. Semini, H. Kogler, R. Scheidl, and D. G. Caldwell, "Power hydraulics–switched mode control of hydraulic actuation," in *Proc. IEEE/RSJ Int. Conf. Intell. Robots Syst.*, Oct. 2010, pp. 3031–3036.

[16] H. Kogler, R. Scheidl, and M. Ehrentraut, "A simulation model of a hydraulic buck converter based on a mixed time frequency domain iteration," in *Proc. ASME/BATH Symp. Fluid Power Motion Control*, Sarasota, FL, USA, Oct. 2013, pp. 1–10.

[17] T. H. Ho and K. K. Ahn, "Design and control of a closed-loop hydraulic energy-regenerative system," *Autom. Construct.*, vol. 22, pp. 444–458, Mar. 2012.

[18] H. H. Triet and K. K. Ahn, "Comparison and assessment of a hydraulic energy-saving system for hydrostatic drives," *Proc. Inst. Mech. Eng., I, J. Syst. Control Eng.*, vol. 225, no. 1, pp. 21–34, Feb. 2011.

[19] T. H. Ho and K. K. Ahn, "Modeling and simulation of hydrostatic transmission system with energy regeneration using hydraulic accumulator," *J. Mech. Sci. Technol.*, vol. 24, no. 5, pp. 1163–1175, May 2010.

[20] F. Wang, L. Gu, and Y. Chen, "A hydraulic pressure-boost system based on high-speed on–off valves," *IEEE/ASME Trans. Mechatronics*, vol. 18, no. 2, pp. 733–743, Apr. 2013.

[21] P. A. J. Achten, T. van den Brink, J. van den Oever, J. Potma, M. Schellekens, G. Vael, M. van Walwijk, and B. Innas, "Dedicated design of the hydraulic transformer," in *Proc. IFK3*, 2002, pp. 233–248.

[22] S. Lee and P. Y. Li, "Passivity based backstepping control for trajectory tracking using a hydraulic transformer," in *Proc. ASME/BATH Symp. Fluid Power Motion Control*, Oct. 2015, pp. 1–10.

[23] W. Shen, J. Jiang, X. Su, and H. R. Karimi, "A new type of hydraulic cylinder system controlled by the new-type hydraulic transformer," *Proc. Inst. Mech. Eng., C, J. Mech. Eng. Sci.*, vol. 228, no. 12, pp. 2233–2245, Aug. 2014.

[24] E. Bishop, "Digital hydraulic transformer = Digital hydraulic muscle," in *Proc. 52nd Nat. Conf. Fluid Power*, Las Vegas, NV, USA, 2011, pp. 649–656.

[25] Y. Xue, J. Shang, J. Yang, and Z. Wang, "A new converter for improving efficiency of multi-actuators fluid power system," *J. Mech. Sci. Technol.*, vol. 30, no. 5, pp. 2273–2281, May 2016.

[26] F. R. Xu, "Calculation of frictional force of O-ring," *Lubrication Eng.*, vol. 17, no. 8, pp. 32–34, Aug. 1989.

[27] A. K. Ellman and R. A. Piche, "A modified orifice flow formula for numerical simulation," *J. Dyn. Syst., Meas., Control*, vol. 121, no. 4, pp. 721–724, 1996.

[28] S. J. Yang, N. Wang, and Q. Wang, "Experimental study on flow characteristics of high—Speed on-off valve," *Mach. Tools Hydraulic*, vol. 43, no. 23, pp. 1–3, 2015.

[29] H. B. Jiang and J. Ruan, "A new type of high-flow high-speed on-off valve," *Chin. Hydraul. Pneum.*, vol. 14, no. 11, pp. 96–99, 2013, doi: 10.11832/j.issn.1000-4858.2013.11.026.

GUOHENG WU received the B.A.Sc. and M.A.Sc. degrees in mechanical engineering from the National University of Defense Technology, Changsha, China, in 2013 and 2015, respectively, where he is currently pursuing the Ph.D. degree with the Department of Mechanical Engineering.

JUNHONG YANG received the B.A.Sc. degree from Xi'an Jiaotong University, Xi'an, China, in 2000, and the M.A.Sc. and the Ph.D. degrees in mechanical engineering from the National University of Defense Technology, Changsha, China, in 2002 and 2007, respectively. He is currently with China Minsheng Drawin Intelligent Equipment Technology Company Limited.

JIANZHONG SHANG received the B.A.Sc. and M.A.Sc. degrees from the National University of Defense Technology, Changsha, China, in 1988 and 1991, respectively, and the Ph.D. degree in mechanical design and theory from the Huazhong University of Science and Technology, Wuhan, China, in 2006. He is currently a Professor with the Department of Mechanical Engineering, National University of Defense Technology.

ZIRONG LUO received the B.A.Sc. and M.A.Sc. degrees from the Huazhong University of Science and Technology, Wuhan, China, in 1999 and 2003, respectively, and the Ph.D. degree from the National University of Defense Technology, Changsha, China, in 2009. He is currently a Professor with the Department of Mechanical Engineering, National University of Defense Technology.

TENGAN ZOU received the M.A.Sc. and Ph.D. degrees in mechanical engineering from the National University of Defense Technology, Changsha, China, in 2009 and 2014, respectively. He is currently a Lecturer with the College of Intelligence Science and Technology, National University of Defense Technology.

DELEI FANG received the B.A.Sc. degree from the Hebei University of Science and Technology and the M.A.Sc. degree from Yanshan University, Hebei, China, in 2014, and the Ph.D. degree from the National University of Defense Technology, Changsha, China, in 2018, respectively. He is currently a Lecturer with the Tianjin University of Science and Technology.